

Luminescence of manganese and chromium ions in spinel hosts

© N.M. Khaidukov¹, M.N. Brekhovskikh¹, N.Yu. Kirikova², V.A. Kondratyuk², V.N. Makhov^{2,¶}

¹Kurnakov Institute of General and Inorganic Chemistry, Russian Academy of Sciences, 119991 Moscow, Russia

²Lebedev Physical Institute, Russian Academy of Sciences, 119991 Moscow, Russia

¶ e-mail: makhovvn@lebedev.ru

Received November 23, 2022

Revised December 09, 2022

Accepted December 12, 2022.

Single-phase ceramic samples of MgAl_2O_4 , ZnAl_2O_4 and LiAl_5O_8 spinels containing manganese or chromium ions have been synthesized by a high-temperature solid-state reactions method. It has been shown that the luminescence properties of the synthesized phosphors, in particular, the appearance of intense red luminescence from Mn^{4+} ions, as well as the magnitude of inhomogeneous line broadening in the luminescence spectra of Mn^{4+} and Cr^{3+} ions depend on the degree of cation inversion, which provides the charge compensation for stabilizing Mn^{4+} ions in the octahedral sites of the spinel structures upon the substitution of Al^{3+} ions, simultaneously resulting in disordered spinel crystal structures.

Keywords: spinel, inversion, manganese and chromium ions, red phosphor.

DOI: 10.61011/EOS.2023.04.56350.56-22

Introduction

To date, a large number of practical phosphors and laser materials as well have been developed and studied, in which manganese and chromium ions are optically active ions. Nevertheless, studies of the luminescence features of these ions in matrices of various types are being actively continued. In particular, in recent years, a lot of papers have been devoted to the search and study of new red phosphors for LED sources of warm white light, i.e. for white light LED lamps with high color rendering index, in which Mn^{4+} [1–5] ions provide red luminescence. In addition, in recent years the development of phosphors emitting in the red and far red ranges of the spectrum have been very popular, in particular, phosphors based on Mn^{4+} and Cr^{3+} ions, for agrotechnical applications, namely, to stimulate plant growth in greenhouses, since in these spectral ranges there are the absorption bands of chlorophylls A and B, as well as phytochrome (P_R and P_{FR}), which are responsible for plant growth [5,6]. On the other hand, since the optical properties of manganese and chromium ions have been studied in a variety of compounds and it is believed that the interpretation of these properties is usually quite transparent, studies of the luminescent properties of these ions can be considered as a spectroscopic probe for studying the features of the crystal structure of matrices in which these ions are introduced.

The scheme of energy levels of the Mn^{4+} and Cr^{3+} ions is determined by the well-known Tanabe-Sugano diagram for ions with the d^3 electronic configuration located in the ideal octahedral site [7]. The diagram shows that the two main broad absorption bands of these ions are due to the spin-allowed transitions ${}^4A_2 \rightarrow {}^4T_2$ and ${}^4A_2 \rightarrow {}^4T_1$, while the

spin-forbidden ${}^2E \rightarrow {}^4A_2$ transitions are responsible for the narrow-band luminescence. The spectral position of the absorption and luminescence bands of the Mn^{4+} and Cr^{3+} ions strongly depends on the composition of the host, which allows to vary the luminescent properties of phosphors based on these ions for specific applications. However, from the point of view of practical application, it is obvious that oxide matrices are more preferable.

One of the oxide matrices frequently used to create phosphors are compounds with a spinel structure. Crystal structure of spinel is based on a densely packed cubic oxygen sublattice, and cations can occupy two types of crystallographic positions: with tetrahedral and octahedral oxygen ion surroundings (Fig. 1) [8]. This structure of the crystal lattice allows to introduce optically active ions with various charge states into the spinel host. In particular, manganese ions can enter into the spinel host with the charge 2+, 3+, and 4+.

In this paper, a comparative feature analysis of the luminescent properties of three types of ceramic phosphors based on three compounds with a spinel structure is carried out: MgAl_2O_4 , ZnAl_2O_4 and LiAl_5O_8 , doped with manganese and chromium ions, including the temperature dependences of the luminescence spectra.

Samples and experimental procedure

Ceramic samples of three aluminate compounds, namely, MgAl_2O_4 , ZnAl_2O_4 and LiAl_5O_8 , doped with manganese or chromium ions (0.05–0.2 at% relative to aluminum ions), were obtained as a result of high-temperature solid-phase synthesis upon interaction of Al_2O_3 (purity 99.99%) and

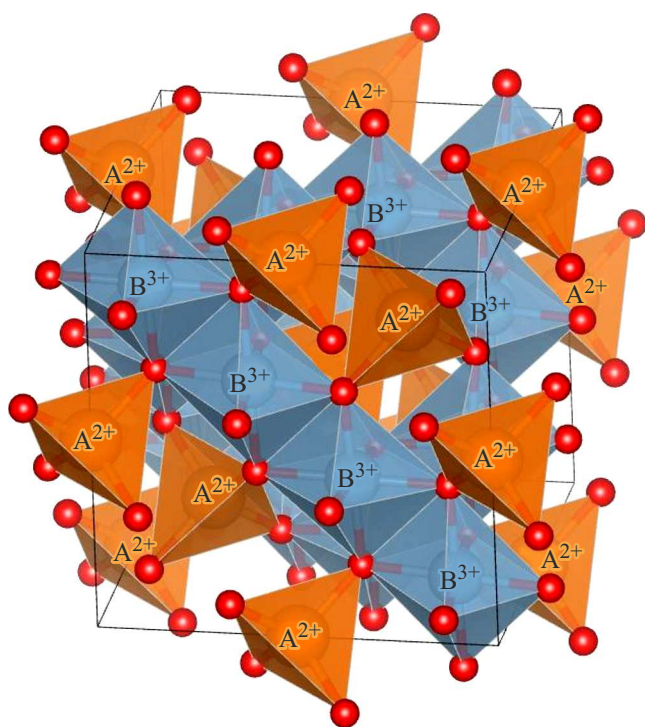


Figure 1. Crystal structure of spinel. In this example, the divalent cations A^{2+} occupy tetrahedral positions, and the trivalent cations B^{3+} occupy octahedral sites in AB_2O_4 , as is observed in the structures of normal spinels $MgAl_2O_4$ and $ZnAl_2O_4$.

$MgCO_3$ (99.99%), $ZnCO_3$ (99.99%), Li_2CO_3 (99.99%) respectively, as well as MnO_2 (99.999%) or Cr_2O_3 (99.99%). For the synthesis of $MgAl_2O_4$ and $ZnAl_2O_4$ the initial reagents were mixed in stoichiometric ratios, and for the synthesis of $LiAl_5O_8$, mixtures with a molar ratio of the starting components Al_2O_3/Li_2CO_3 equal to 2.5 were used, i.e. the initial mixture contained two times more Li^+ ions compared to the stoichiometric composition $LiAl_5O_8$, taking into account the high volatility of Li_2O . Powder mixtures were uniaxially pressed in a stainless steel mold at a pressure of approximately 150 MPa into pellets 10 mm in diameter and 2 mm thick. The pellets were subjected to preliminary successive low-temperature annealing in air at temperatures of 500, 700, and 900 °C for 4 h in corundum crucibles. Studies of the crystal structure and luminescent properties were carried out for the samples further subjected to successive high-temperature annealing at temperatures of 1000, 1100, 1200, and 1300 °C for 4 h in air. The tablets were ground and pressed again before each annealing. Besides, before the last annealing, 3 mas% H_3BO_3 was added to the sample as a flux. It should be noted that such a multistage annealing technique allowed to synthesize $MgAl_2O_4$ ceramics containing a significant fraction of the normal (non-inverse) spinel phase [9]. In some cases, the synthesis was carried out without preliminary low-temperature annealing, and the annealing time was increased to 20 h. Some samples were subjected to additional

annealing in a reducing atmosphere of carbon monoxide in graphite crucibles. Some details of the annealing of specific samples are presented below in the corresponding sections describing the results of spectroscopic studies.

The structure and phase purity of the samples were studied by X-ray powder diffraction on a Bruker D8 Advance X-ray diffractometer with monochromatic $CuK\alpha$ radiation. The identification of the synthesized compounds, as well as the indexing of X-ray diffraction patterns, was carried out in the EVA software package (Bruker) using the COD database. The results of X-ray diffraction analysis confirm that the X-ray diffraction patterns of the synthesized ceramic samples are indicated in the cubic syngony, and the ceramics have a spinel structure. The lattice parameters of $LiAl_5O_8$, $MgAl_2O_4$ and $ZnAl_2O_4$ synthesized under different conditions varied within the limits 7.908–7.925, 8.07–8.09 and 8.08–8.10 Å respectively. Any regularity in the change in the lattice constant depending on the synthesis conditions are not traced.

The luminescence spectra of the synthesized samples were studied on a setup assembled on the basis of an MDR-12 high-aperture monochromator, in which a blue (455 nm) light-emitting diode (Mightex) was used as a source of excitation radiation. A small-sized flow-type nitrogen cryostat of a special design [10] was used for low-temperature measurements. The temperature was controlled using a calibrated PT100Ω platinum thermoresistance. The luminescence excitation spectra and luminescence kinetics were recorded on a CM 2203 spectrofluorimeter (Solar, Minsk).

Results and discussion

$MgAl_2O_4$

In the crystal structure of the normal spinel $MgAl_2O_4$, belonging to the space group (sp. gr.) $Fd\bar{3}m$, each divalent cation (Mg^{2+}) is located in the center of an undistorted tetrahedron (local symmetry group T_d), and each trivalent cation (Al^{3+}) is located in an octahedron with a trigonal distortion (symmetry group D_{3d}). However, an inversion is possible in the spinel structure; some of the divalent cations can be in the octahedral site, and some of the trivalent cations — in the tetrahedral position. As a result, cationic disordering is created in both octahedral and tetrahedral positions due to differences in ionic radii.

As a result of the synthesis of $MgAl_2O_4$ samples doped with manganese ions using the multistage annealing procedure described above, a phosphor is obtained that emits pure red luminescence of Mn^{4+} ions with a peak at 651 nm, i.e. such a phosphor contains manganese ions exclusively in the 4+ charge state (Fig. 2) [11–13]. It is obvious that Mn^{4+} ions replace Al^{3+} ions in octahedral sites in $MgAl_2O_4$, taking into account that the ionic radii of Mn^{4+} (0.53 Å) and Al^{3+} (0.535 Å) [14] in an octahedron are almost the same, as well as the generally accepted statement that Mn^{4+} ions can be stabilized in the crystal lattice and

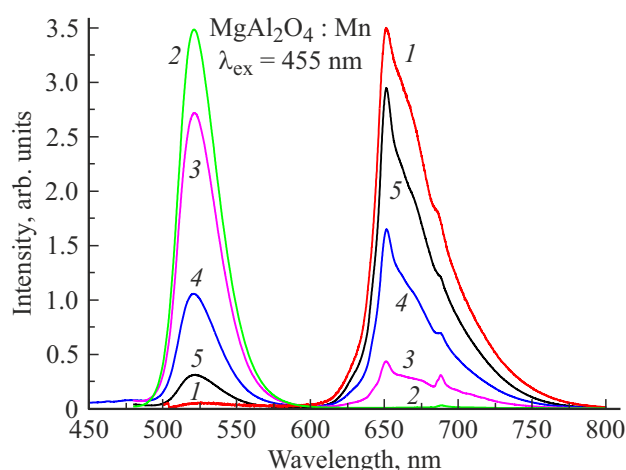
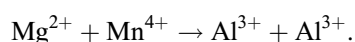


Figure 2. Luminescence spectra of manganese ions in MgAl_2O_4 samples synthesized under different conditions, in particular, the (1) — sample using a multistage annealing procedure at 500, 600, 700, 1000, 1200, and 1300°C in air, sample (2) — in a reducing CO atmosphere, samples (3–5) — synthesized in air at temperatures of 1000, 1200, and 1300°C, respectively without pre-annealing at lower temperatures.

exhibit luminescence only in an octahedral environment. As can be seen from Fig. 2, the luminescence spectrum of Mn^{4+} ions is not narrow-band, as might be expected based on the scheme of energy levels of the Mn^{4+} ion. However, since tetravalent manganese ions replace Al^{3+} ions with charge 3+, charge compensation is necessary to stabilize Mn^{4+} ions in the crystal host structure. As noted above, a characteristic property of magnesium spinel is the opportunity of the existence of a significant degree of inversion, i.e. Mg^{2+} ions can replace Al^{3+} ions in the octahedron, and the charge compensation in this spinel occurs as a result of the heterovalent substitution process:



Meanwhile, all lines in the luminescence spectrum experience a strong nonhomogeneous broadening due to the disorder of the structure caused by the inversion. Thus, the peak at 651 nm in the luminescence spectrum of $\text{MgAl}_2\text{O}_4:\text{Mn}^{4+}$ corresponds to the nonhomogeneously broadened zero-phonon line (ZPL) of the ${}^2E \rightarrow {}^4A_2$ transition in the Mn^{4+} ion, the long-wavelength wing of the spectrum — to Stokes vibronic lines, and shortwavelength one — to anti-Stokes vibronic lines.

Annealing of spinel MgAl_2O_4 containing manganese ions in a reducing atmosphere results in a green phosphor, in which manganese ions having a charge of 2+ and replacing Mg^{2+} ions in the tetrahedral positions of the structure are responsible for luminescence (Fig. 2). Under changing synthesis conditions, for example, in the absence of a low-temperature multistage annealing procedure, two-color phosphors are obtained with red and green luminescence bands due to tetravalent and divalent manganese ions,

respectively, with a different ratio of the intensities of the red and green luminescence bands, depending on the synthesis conditions.

Let us note that in all spectra presented in this article, luminescence excitation is carried out at a wavelength of 455 nm, corresponding to the emission of a standard blue LED.

Both the green band and the red band of the luminescence of the Mn^{2+} and Mn^{4+} ions in spinel MgAl_2O_4 have sufficiently high temperature stability [11]. In particular, the green luminescence intensity of the $\text{MgAl}_2\text{O}_4:\text{Mn}^{2+}$ phosphor annealed in a carbon monoxide reducing atmosphere decreases by 2 times at 465 °C as compared to the intensity at room temperature. The temperature stability of the red luminescence of the phosphor $\text{MgAl}_2\text{O}_4:\text{Mn}^{4+}$ is somewhat worse, but also acceptable: the intensity decreases by 2 times at a temperature of 175 °C.

Thus, both green and red phosphors based on spinel MgAl_2O_4 doped with manganese ions may be of practical interest. The property of different temperature dependences of the intensities of red (Mn^{4+}) and green (Mn^{2+}) luminescence in MgAl_2O_4 can potentially be used as a method of luminescent thermometry, in which the measured temperature-dependent parameter will not be the intensity of some single luminescence band, but the ratio of the intensities of red and green luminescence.

Calculated color coordinates (CIE1931) for the spectra of luminescence of manganese ions in MgAl_2O_4 are $x = 0.18$, $y = 0.75$ for green luminescence of Mn^{2+} and $x = 0.72$, $y = 0.28$ for red luminescence of Mn^{4+} [11]. Both luminescence bands are effectively excited in the blue spectral range, which allows to apply the canonical three-color (RGB: red, green, blue) method for creating LED sources of warm white light based on a combination of a blue LED (455 nm) and a single-phase two-color phosphor $\text{MgAl}_2\text{O}_4:\text{Mn}$ with an optimal ratio of the intensities of the green and red luminescence bands.

Cr^{3+} ions, when introduced into the spinel MgAl_2O_4 host, apparently replace trivalent aluminum ions, which does not require charge compensation provided by cation inversion in case of doping with Mn^{4+} ions. Therefore, in this host obtaining of a narrow-band luminescence spectrum of Cr^{3+} ions can be expected. Indeed, in the natural spinel minerals MgAl_2O_4 , narrow ZPL and vibronic lines are observed in the luminescence spectrum of Cr^{3+} [15], i.e. in nature, the formation of spinels is possible, in which there is practically no inversion of cations. However, samples of MgAl_2O_4 obtained under laboratory conditions are always characterized by a certain degree of cation inversion, i.e. in such samples, there is disorder in both the tetrahedral and octahedral sites of the structure, which leads to a strong nonhomogeneous broadening of lines in the luminescence spectrum, including Cr^{3+} ions, although, possibly, not to the same extent as in case of Mn^{4+} ions. The Cr^{3+} luminescence spectra of the MgAl_2O_4 spinel obtained by multiple sequential annealing have features similar to those for the Mn^{4+} ion, but shifted to the long wavelength range,

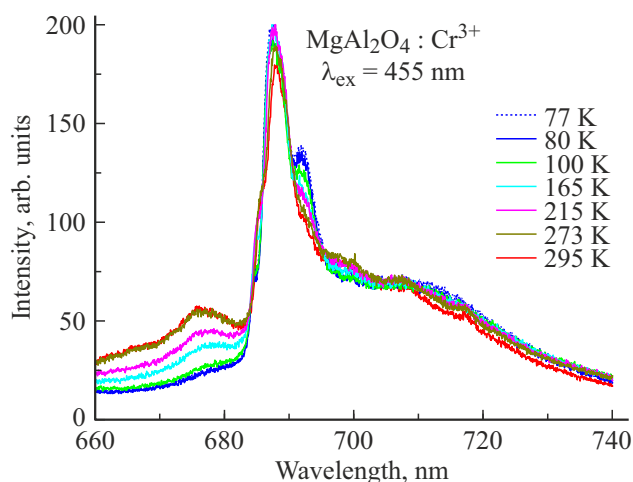


Figure 3. Luminescence spectra of $\text{MgAl}_2\text{O}_4:\text{Cr}^{3+}$ measured at different temperatures.

i.e., demonstrate nonhomogeneously broadened ZPLs with a peak at 688 nm, as well as Stokes and anti-Stokes vibronic bands, the latter disappearing with decreasing temperature (Fig. 3).

Spinel MgAl_2O_4 can be co-doped with Mn^{4+} and Cr^{3+} ions, potentially giving a broad emission spectrum of the phosphor in the red and far red regions. Lamps consisting of a blue LED and a blue-excited phosphor based on spinel MgAl_2O_4 containing ions Mn^{4+} and Cr^{3+} may be of great practical interest for artificial lighting in greenhouses, since the emission spectrum of such a lamp will very well correspond to the absorption spectra of chlorophylls and phytochrome.

ZnAl₂O₄

Zinc aluminate has a crystal structure similar to that of magnesium aluminate, i.e. belongs to the structural type of spinel, in the structure of which aluminum ions occupy octahedral sites, and zinc ions — tetrahedral ones. X-ray diffraction patterns of two types of spinels MgAl_2O_4 and ZnAl_2O_4 are, of course, identical in structure, but the intensities of some peaks differ greatly, since Zn is a much heavier element than Mg or Al (Fig. 4). Along with this, the inversion of cations in the ZnAl_2O_4 structure should also significantly change the shape of the X-ray diffraction pattern, which can be seen in Fig. 4 from a comparison of the X-ray patterns of the normal and inverse ZnAl_2O_4 spinel modeled using the VESTA [16] software, in which both tetrahedral and octahedral sites are 33% occupied by Zn^{2+} ions and 67% by Al^{3+} ions. It should also be noted that the X-ray diffraction pattern of the ZnAl_2O_4 spinel synthesized by us is in good agreement with the X-ray diffraction pattern of the normal spinel ZnAl_2O_4 from the database [17].

Regardless of the fact that the procedure for the synthesis of zinc spinel ceramics doped with manganese ions was the same as for magnesium spinel, the luminescence spectra

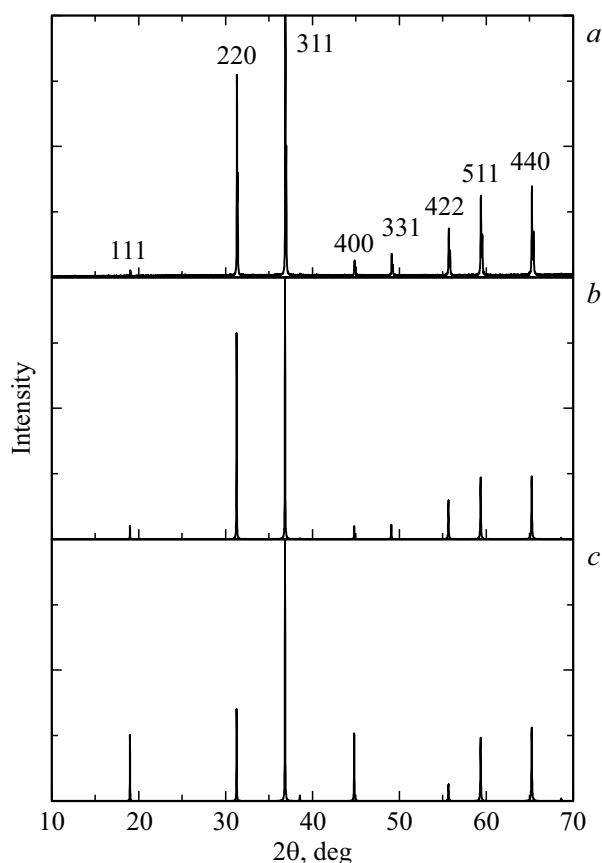


Figure 4. (a) Experimental X-ray diffraction pattern of the synthesized spinel sample ZnAl_2O_4 ; (b) X-ray diffraction pattern of ZnAl_2O_4 spinel from the database [17]; (c) simulated X-ray diffraction pattern of inverse spinel ZnAl_2O_4 .

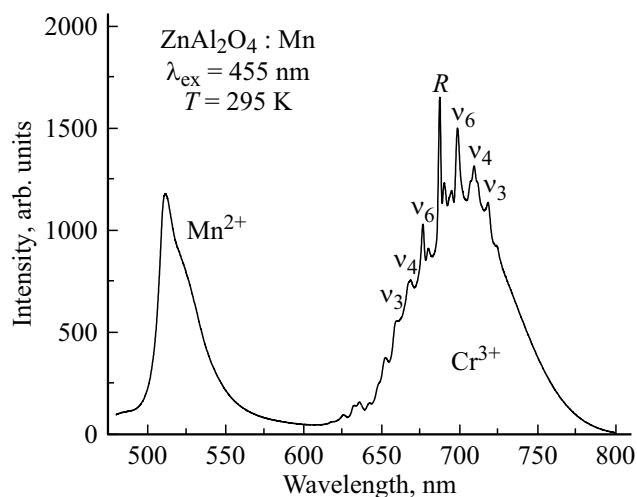


Figure 5. Luminescence spectra of Mn^{2+} and Cr^{3+} ions in ZnAl_2O_4 spinel synthesized by successive annealing at 500, 600, 700, 1000, 1200, and 1300°C.

of the synthesized ZnAl_2O_4 samples did not contain luminescence bands that can be attributed to Mn^{4+} ions [12]. On the other hand, the luminescence spectrum exhibits a

set of narrow lines characteristic of Cr^{3+} ions (Fig. 5). The same spectrum is recorded for undoped samples, in which chromium ions are present as an uncontrolled impurity.

Thus, it is not possible to stabilize the Mn^{4+} ions in the octahedral sites of the structure of zinc spinel. The reason for this is that, unlike magnesium spinel, a characteristic feature of zinc spinel is that the degree of inversion (the fraction of tetrahedral positions occupied by Al^{3+} ions) is very low and does not exceed 0.055 in the limiting case [18]. This feature does not allow to provide charge compensation for the substitution of Mn^{4+} ions for triply charged aluminum ions in octahedral sites. However, green luminescence (~ 515 nm) of Mn^{2+} ions replacing zinc ions in tetrahedra is always present.

Due to the low degree of inversion, i.e. the absence of lattice disorder, the fine structure of the spectra is clearly identified in the luminescence spectrum of Cr^{3+} ions in ZnAl_2O_4 : ZPL of a purely electronic transition ${}^2E \rightarrow {}^4A_2$ (the so-called *R*-line), as well as 3 Stokes and 3 anti-Stokes vibronic lines corresponding to three modes of odd-parity vibrations ν_3 , ν_4 , and ν_6 of the CrO_6^{9-} octahedron [12]. It should be noted that the ZPL and vibronic line intensities are comparable, since this electronic transition is parity and spin forbidden, and the octahedral polyhedron in the structure of zinc and magnesium spinels, although distorted (trigonal distortion, symmetry group D_{3d}), has a center of symmetry. Therefore, the probability of a purely electronic transition is small, and the vibronic lines have a relatively high intensity. There are other weaker ZPLs in the spectrum, which are usually attributed to the luminescence of more complex chromium centers, for example, pairs of chromium ions $\text{Cr}^{3+}-\text{Cr}^{3+}$.

Measurements of the temperature dependence of the spectra structure showed the typical behavior of its features with decreasing temperature, namely, the disappearance of the anti-Stokes vibronic lines, as well as the narrowing and spectral shift of the ZPL. In low-temperature

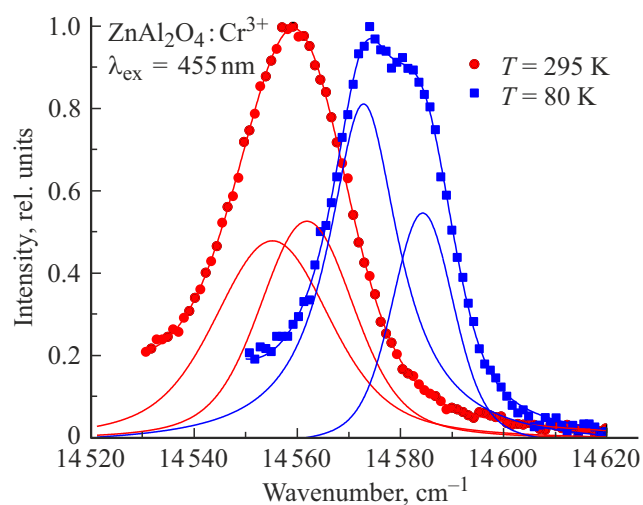


Figure 6. ZPL splitting for the electronic transition ${}^2E \rightarrow {}^4A_2$ for ions Cr^{3+} in the spinel ZnAl_2O_4 .

measurements with a fairly high spectral resolution, ZPL splitting can also be seen (Fig. 6). The observed two luminescence lines, denoted in the literature as R_1 and R_2 , are due to the ${}^2E \rightarrow {}^4A_2$ electronic transition in the Cr^{3+} ion from two sublevels \bar{E} and $2\bar{A}$ of the 2E state, whose splitting occurs as a result of the joint action of the distortion of the octahedral symmetry of the crystal field around the chromium ion and spin-orbit interaction [19]. The value of this splitting in the ZnAl_2O_4 host is small ($\Delta E_{1,2} \sim 10$ cm^{-1}) [15] and is comparable to the linewidths in the synthesized samples. Therefore, it is difficult to perform a quantitative analysis of the temperature dependence of the spectral position and linewidth here.

LiAl_5O_8

Lithium aluminate LiAl_5O_8 has a spinel-type crystal structure (sp. gr. $P4_132$), in which the Li^+ and Al^{3+} ions in the 1:3 ratio orderly occupy two types of octahedral positions: $4b$ and $12d$ respectively. The remaining Al^{3+} ions occupy the tetrahedral position $8c$. However, it can be expected that different degrees of inversion are possible in the structure of this spinel for the distribution of Li^+ and Al^{3+} cations over octahedral sites in the LiAl_5O_8 structure. The Mn^{4+} and Cr^{3+} ions replace in LiAl_5O_8 Al^{3+} ions in the octahedral sites, which have rhombic distortion in the LiAl_5O_8 structure (local symmetry C_2) [20,21].

The results of X-ray diffraction analysis confirmed that ceramic samples annealed in the 1000–1300°C temperature range are identified as the LiAl_5O_8 compound with the ordered arrangement of the Li^+ and Al^{3+} ions in the octahedral and tetrahedral lattice sites described above (Fig. 7). However, the cubic lattice parameter a , determined from the interplanar spacing $d(440)$, decreases with increasing temperature and (or) annealing duration and reaches 7.908 Å for ceramics subjected to sufficiently long-term annealing at 1300 °C. This value exactly corresponds to the crystal lattice parameter for a single-crystal LiAl_5O_8 , i.e. for the ideally stoichiometric composition LiAl_5O_8 [20].

The luminescence spectra of manganese doped LiAl_5O_8 samples subjected to annealing at different temperatures and durations (Fig. 8) show that the intensity of the characteristic red luminescence of Mn^{4+} ions (peak at 662 nm), clearly observed in samples synthesized at $\sim 1000^\circ\text{C}$, decreases with an increase in the temperature and duration of annealing, and the luminescence of Mn^{4+} practically disappears when the stoichiometric composition LiAl_5O_8 [22,23] is formed according to the annealing conditions.

As in the two aluminates with a spinel structure considered above, in LiAl_5O_8 ions Mn^{4+} should replace Al^{3+} ions in octahedral sites, and charge compensation should be provided to stabilize Mn^{4+} ions in the lattice. Taking into account the excess amount of Li^+ ions in the mixture of initial reagents, it is natural to assume that the charge compensation is provided by the mechanism

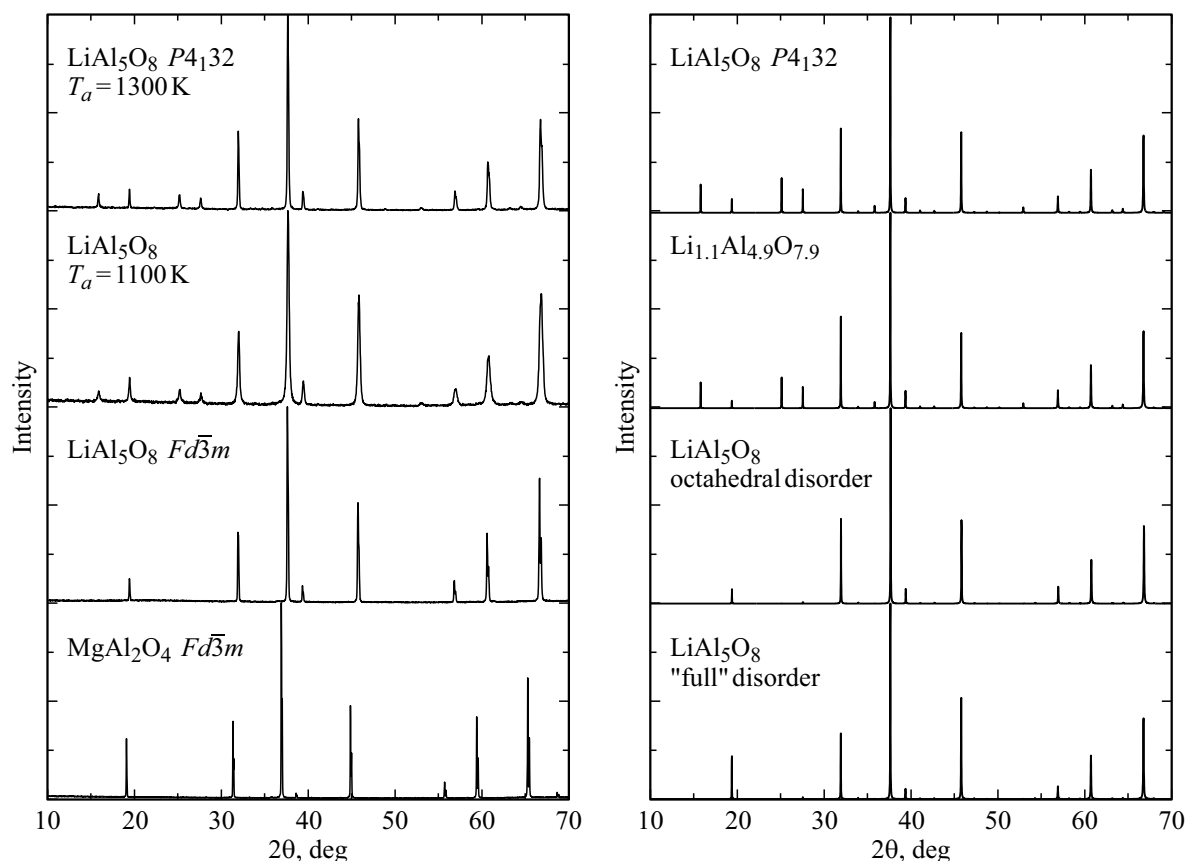


Figure 7. Left panel: experimental X-ray diffraction patterns of „completely“ ordered (long-term annealing at 1300°C), „partially“ disordered (annealed at 1100°C for 4 h), and „completely“ disordered LiAl_5O_8 , as well as spinel MgAl_2O_4 . Right panel: X-ray diffraction pattern „of the completely“ ordered LiAl_5O_8 from the database [17], X-ray diffraction patterns of the LiAl_5O_8 compound modeled using the VESTA [16] software with a certain (10%) excess amount of Li^+ ions replacing Al^{3+} ions in the octahedral lattice sites, and also in the presence of a different degree of disorder, i.e. with „statistical“ distribution of Al^{3+} and Li^+ ions either only over octahedral sites or over all cation sites.

of cation inversion, i.e. substitution of some Al^{3+} ions adjacent to Mn^{4+} by Li^+ ions. Compounds with a certain excess of lithium are unstable and, as the temperature and/or duration of annealing increase, they lose Li^+ ions, transforming into the stoichiometric compound LiAl_5O_8 , in which there is no inversion and, accordingly, there is no charge compensation mechanism. Meanwhile, because of the smaller value of the ionic radius Al^{3+} (0.535 Å) as compared to Li^+ (0.76 Å) [14], the lattice constant decreases. Thus, the luminescence of Mn^{4+} ions can be obtained only in case of the presence of inversion, i.e. disorder in the spinel structure LiAl_5O_8 , which, among other things, leads to nonhomogeneous line broadening in the spectra. Basically, the intensity of the red luminescence of Mn^{4+} ions can be used as a criterion for the degree of order in the structure of the compound LiAl_5O_8 .

As an additional experiment, the stoichiometric sample LiAl_5O_8 doped with manganese ions, i.e. the sample, which did not show the luminescence of the Mn^{4+} ions, was annealed again at 1300°C with the addition of an excess amount of lithium. The obtained samples, as expected,

showed the presence of sufficiently bright red luminescence of Mn^{4+} ions. However, the X-ray diffraction pattern of the obtained sample turned out to be completely different and did not correspond to the stoichiometric compound LiAl_5O_8 [23]. As it was shown in [24], the compound LiAl_5O_8 undergoes a phase transition at a temperature of about 1300°C, transforming from the ordered structure (sp. gr. $P4_132$) described above to disordered, in which the Al^{3+} and Li^+ ions statistically, i.e. randomly occupy cationic sites in the lattice LiAl_5O_8 . In this case, the lattice symmetry changes to another type, which is characteristic of the spinels MgAl_2O_4 and ZnAl_2O_4 considered above (sp. gr. $Fd\bar{3}m$). The presence of such a disorder, i.e. essentially, the presence of a high degree of cation inversion provides charge compensation for the Mn^{4+} ions in the samples obtained in this way.

Fig. 7 (left panel) compares the experimental X-ray diffraction patterns of „completely“ ordered (long-term annealing at 1300°C), „partially“ disordered (annealing at 1100°C for 4 h) and obtained in an additional experiment „completely“ disordered LiAl_5O_8 , as well as MgAl_2O_4

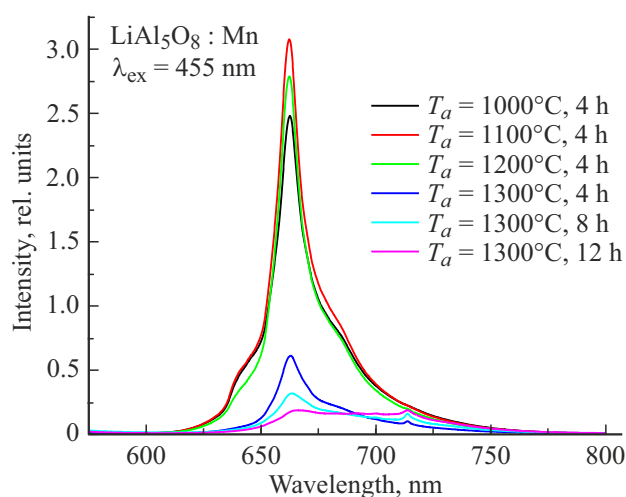


Figure 8. Luminescence spectra of Mn^{4+} ions in LiAl_5O_8 ceramic samples synthesized at annealing temperatures of 1000, 1100, 1200, and 1300°C and annealing times of 4, 8, and 12 h.

spinel for comparison. It can be seen that the X-ray diffraction patterns for completely and partially ordered structures are practically the same. Therefore, the phase identification software, when compared with the database, identifies the structure of all such samples as an ordered spinel LiAl_5O_8 . It can also be seen that the X-ray diffraction patterns of the completely disordered LiAl_5O_8 and spinels MgAl_2O_4 are very similar in structure, since their lattices have the same type of symmetry.

Using the VESTA software, X-ray diffraction patterns of the compound LiAl_5O_8 were simulated with a certain (10%) excess amount of Li^+ ions replacing Al^{3+} ions in the octahedral sites of the structure, as well as in the presence of various degrees of disorder (Fig. 7, right panel). It can be seen in the calculated X-ray diffraction patterns that a slight excess of the amount of lithium ions in comparison with the stoichiometry does not actually change the shape of the X-ray diffraction pattern, while disordering, i.e. the statistical distribution of lithium and aluminum ions over cationic positions radically changes the shape of the X-ray pattern, which becomes similar to X-ray patterns for another type of cubic lattice symmetry, and the experimental X-ray pattern of disordered LiAl_5O_8 better corresponds to the calculated X-ray pattern with the statistical distribution of Al^{3+} and Li^+ ions only over octahedral sites.

Doping of the LiAl_5O_8 host with Cr^{3+} ions replacing Al^{3+} ions does not require charge compensation, and the luminescence spectra of our synthesized samples of LiAl_5O_8 ceramics doped with Cr^{3+} ions demonstrate a shape typical of Cr^{3+} ions with two narrow ZPL: at ~ 714 nm (more intense) and ~ 700 nm (Fig. 9) [10]. As in the case of ZnAl_2O_4 host, it can be assumed that these luminescence lines are due to the ${}^2E \rightarrow {}^4A_2$ electronic transition in the ion from two sublevels of the 2E state, the splitting of which occurs as a result of distortion of the octahedral symmetry

of the crystal field around the chromium ion, i.e., these are the lines designated in the literature as R_1 and R_2 . However, it should be noted that the energy distance between lines in the LiAl_5O_8 ($\sim 270 \text{ cm}^{-1}$ at 295 K) significantly exceeds the splitting observed in many other matrices ($\sim 29 \text{ cm}^{-1}$ in Al_2O_3 [25,26], $\sim 20 \text{ cm}^{-1}$ in YAG [27–29], $\sim 10 \text{ cm}^{-1}$ in spinels MgAl_2O_4 and ZnAl_2O_4 [30]), which may indicate a significantly greater distortion of the environment of Cr^{3+} ions in the LiAl_5O_8 structure compared to other matrices, due to the lower symmetry of the position for Al^{3+} ions replaced by Cr^{3+} ions in the LiAl_5O_8 structure, in comparison with other matrices, namely, instead of the trigonal D_{3d} , there is orthorhombic C_2 symmetry of the optical Cr^{3+} -center [31]. Note that there is an example of a host (Ga_2O_3) in which the splitting value ($\sim 147 \text{ cm}^{-1}$ [32]) is comparable to that observed in the host LiAl_5O_8 . On the other hand, these two ZPL can be referred to as two nonequivalent chromium centers coupled through the energy transfer [33].

In addition to the narrow ZPL, rather weak vibronic bands are observed in the spectra, and the intensity of the anti-Stokes vibronic lines related to the ZPL at 714 nm, in a certain temperature range is comparable to the ZPL intensity at 700 nm, which makes it difficult to distinguish clearly enough in spectrum the line 700 nm. Note that the weakness of the vibronic lines and, accordingly, the high relative intensity of the ZPL are due to the absence of a center of symmetry near the optical Cr^{3+} center in this host, which increases the probability of a purely electronic transition.

The two energy sublevels resulting from the splitting of the 2E state should be in thermal equilibrium, and, as a result, the temperature dependence of the ratio of the luminescence line intensities due to emission transitions from these two sublevels should be described by the Boltzmann function, which was really obtained when measuring

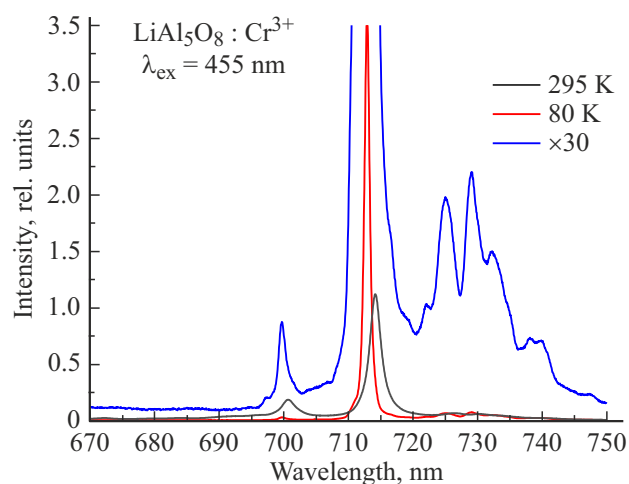


Figure 9. Luminescence spectrum of ceramics $\text{LiAl}_5\text{O}_8:\text{Cr}^{3+}$ (0.1 at.%) measured at 80 and 295 K. The spectrum at 80 K is also shown on an enlarged scale to demonstrate the structure of the vibronic (Stokes) lines related to the ZPL at 714 nm.

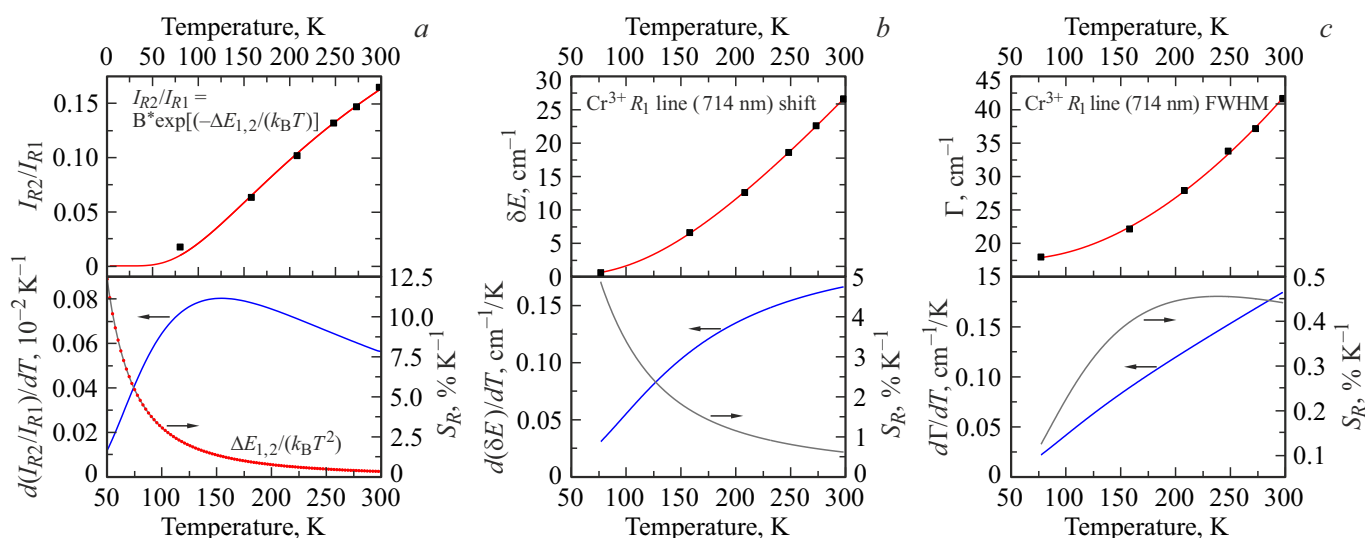


Figure 10. Upper row: temperature dependences of the ZPL intensity ratio at 700 and 714 nm (a), ZPL spectral shift at 714 nm (b), ZPL full width at half maximum at 714 nm (c). The lines show the results of the experimental data approximation (points) by the Boltzmann function (a) and the McComber & Sturge [25] (b and c) formulas. Lower row: temperature dependences of sensitivity (left) and relative sensitivity (right, S_R) of each of the temperature measurement methods.

the temperature dependences of the luminescence spectra of $\text{LiAl}_5\text{O}_8:\text{Cr}^{3+}$ (Fig. 10,a). However, in case of two nonequivalent chromium centers, which are coupled by phonon assisted nonresonant energy transfer, the intensity ratio of the two lines can also be described by the Boltzmann function [34]. Thus, the question of the true nature of these two ZPLs is still open.

In addition to the change in intensity, both ZPLs undergo a spectral shift and a change in width with temperature (Fig. 10, b, c), similar to those observed for similar lines in other matrices, in particular, in ZnAl_2O_4 spinel, as discussed above. Let us note that the spectral resolution in these measurements (0.2 nm) was always much smaller than the linewidth. As can be seen from the figure, the spectral shift and the change in the ZPL width with temperature are described quite well within the well-known model for optical centers in crystals, in which the observed effects are explained by the processes of phonon scattering by an impurity ion [25]. However, the nonhomogeneous ZPL broadening (i.e., the linewidth at zero temperature $\Gamma_0 \sim 20 \text{ cm}^{-1}$) turned out to be noticeably larger than the typical values $\sim 1 \text{ cm}^{-1}$ obtained for other matrices [25–30]. It can be assumed that the larger nonhomogeneous broadening can be associated with an additional distortion of the octahedral position of aluminum in the LiAl_5O_8 structure due to some inversion between the Li^+ and Al^{3+} ions, the degree of which depends on the synthesis conditions.

Thus, in the temperature range 80–295 K under study, three parameters of the Cr^{3+} luminescence spectrum undergo noticeable changes with temperature in the LiAl_5O_8 host: the relative intensity of two ZPLs at 700 and 714 nm, the spectral position of the lines, and the line width. Measurements of each of these three parameters can po-

tentially be used as a non-contact fluorescent thermometry method. The method of thermometry for measuring the ratio of luminescence intensities from two levels in thermal equilibrium is well known. The sensitivity of the method S , defined as the derivative by temperature of the measured parameter, as well as the relative sensitivity S_R , equal to the ratio of sensitivity to the measured parameter value, are quite acceptable in this case (Fig. 10, a). In this method, the relative sensitivity is easily calculated using the formula $S_R = \Delta E_{1,2}/k_B T^2$, where $\Delta E_{1,2}$ — energy distance between levels, T — temperature, k_B — Boltzmann constant. However, since it is difficult to accurately calculate the intensity ratio I_{700}/I_{714} at some temperatures due to the presence of vibronic lines overlapping with ZPL, the accuracy of temperature determination in such measurements may turn out to be low. For the same reason, only the ZPL at 714 nm can actually be used to monitor the temperature by the shift and linewidth. In the studied temperature range, the sensitivity of the temperature measurement method both by line shift and linewidth (Fig. 10, b, c) has a maximum value in the room temperature region and is $\sim 0.2 \text{ cm}^{-1}/\text{K}$ (i.e. $\sim 0.01 \text{ nm}/\text{K}$ for 714 nm). Probably, the value of 0.01 nm can be considered close to the maximum achievable accuracy of measuring the wavelength on spectral instruments. With such an accuracy of spectral measurements, the accuracy of temperature determination (in the area of 295 K) will be $\sim 1 \text{ K}$, which can hardly be considered sufficient for practical use in thermometry.

Conclusions

Single-phase ceramic samples of three aluminate compounds with a spinel structure, namely, MgAl_2O_4 , ZnAl_2O_4 and LiAl_5O_8 , doped with manganese or chromium ions, were successfully synthesized by the method of high-temperature solid-phase reactions. Along with this, effective green (activator ion — Mn^{2+}), red (Mn^{4+}), or two-color (red-green) phosphors, as well as phosphors emitting in far red region (activator ion — Cr^{3+}) can be obtained on the basis of different spinel matrices under various synthesis conditions. However, to create efficient single-color red phosphors doped with Mn^{4+} ions, a special synthesis strategy is required.

Charge compensation for the substitution of Al^{3+} ions in octahedral lattice sites by Mn^{4+} is provided by the inversion of cations having different valence states in spinel compounds. In particular, spinel MgAl_2O_4 , in which a high degree of cation inversion can be achieved, is a promising host for creating a red phosphor containing Mn^{4+} ions, while using the ZnAl_2O_4 spinel host, in which there is almost no inversion between Zn^{2+} and Al^{3+} , it is not possible to obtain a red phosphor with an activator ion Mn^{4+} . Effective red luminescence of Mn^{4+} ions in a spinel host LiAl_5O_8 can be obtained if the synthesis conditions create a structure in which there is an inversion between Li^+ and Al^{3+} ions.

A high degree of cation inversion and, consequently, a large disorder in the spinel structure lead to a strong nonhomogeneous broadening of the ZPL and vibronic lines in the emission spectra of Mn^{4+} and Cr^{3+} . In the studied aluminates with a spinel structure, where the charge compensation for the substitution of Al^{3+} ions by Mn^{4+} ions is provided by cation inversion, the luminescence spectrum of Mn^{4+} is always broadened. Vibronic lines in the emission spectrum of Cr^{3+} can only be identified in spinel compounds with an ordered crystal structure, in particular, in ZnAl_2O_4 and in an ordered host LiAl_5O_8 .

Some of the studied spinel compounds doped with manganese and/or chromium ions can potentially be used as phosphors for various lighting devices, in particular, two-color phosphors — for creating white LED lamps using the canonical three-color (RGB) scheme, phosphors emitting in the red and far red regions for artificial lighting of plants in greenhouses. In addition, a number of synthesized phosphors may be of interest for non-contact luminescent thermometry.

Funding

The paper was supported by the Ministry of Science and Higher Education of the Russian Federation within the state assignments of the Kurnakov Institute of General and Inorganic Chemistry and the Lebedev Physical Institute. The studies were carried out using the equipment of Center for Collective Use of IGIC and LPI.

Conflict of interest

The authors declare that they have no conflict of interest.

References

- [1] Q. Zhou, L. Dolgov, A.M. Srivastava, L. Zhou, Z. Wang, J. Shi, M.D. Dramićanin, M.G. Brik, M. Wu. *J. Mater. Chem. C*, **6**, 2652 (2018). DOI: 10.1039/c8tc00251g
- [2] S. Adachi. *J. Lumin.*, **202**, 263 (2018). DOI: 10.1016/j.jlumin.2018.05.053
- [3] S. Adachi. *ECS J. Solid State Sci. Technol.*, **9**, 016001 (2020). DOI: 10.1149/2.0022001JSS
- [4] Y.H. Kim, J. Ha, W.B. Im. *J. Materials Research and Technology*, **11**, 181 (2021). DOI: 10.1016/j.jmrt.2021.01.011
- [5] S.J. Dhoble, R. Priya, N.S. Dhoble, O.P. Pandey. *J. Lumin.*, **36**, 560 (2021). DOI: 10.1002/bio.3991
- [6] M.H. Fang, G.N.A. De Guzman, Z. Bao, N. Majewska, S. Mahlik, M. Grinberg, R.S. Liu. *J. Mater. Chem. C*, **8**, 11013 (2020). DOI: 10.1039/d0tc02705g
- [7] Y. Tanabe, S. Sugano. *J. Phys. Soc. Jpn.*, **9**, 776 (1954). DOI: 10.1143/JPSJ.9.766
- [8] F. Bosi, C. Biagioni, M. Pasero. *Eur. J. Mineral.*, **3**, 183 (2019). DOI: 10.1127/ejm/2019/0031-2788
- [9] S.P. Feofilov, A.B. Kulinkin, N.M. Khaidukov. *J. Lumin.*, **217**, 116824 (2020). DOI: 10.1016/j.jlumin.2019.116824
- [10] N.M. Khaidukov, K.S. Nikonov, M.N. Brekhovskikh, N.Yu. Kirikova, V.A. Kondratyuk, V.N. Makhov. *Inorganic Materials*, **58** (7), 751 (2022). DOI: 10.1134/S002016852207010X.
- [11] N.M. Khaidukov, M.N. Brekhovskikh, N.Yu. Kirikova, V.A. Kondratyuk, V.N. Makhov. *Russ. J. Inorg. Chem.*, **65** (8), 1135 (2020). DOI: 10.1134/S0036023620080069.
- [12] N.M. Khaidukov, M.N. Brekhovskikh, N.Yu. Kirikova, V.A. Kondratyuk, V.N. Makhov. *Ceram. Int.*, **46**, 21351 (2020). DOI: 10.1016/j.ceramint.2020.05.231
- [13] N. Khaidukov, A. Pirri, M. Brekhovskikh, G. Toci, M. Vannini, B. Patrizi, V. Makhov. *Materials*, **14** (2), 420 (2021). DOI: 10.3390/ma14020420
- [14] R.D. Shannon. *Acta Cryst. A*, **32**, 751 (1976). DOI: 10.1107/S0567739476001551
- [15] D.L. Wood, G.F. Imbusch, R. M. Macfarlane, P. Kisliuk, D.M. Larkin. *J. Chem. Phys.*, **48**, 5255 (1968). DOI: 10.1063/1.1668202
- [16] K. Momma, F. Izumi. *J. Appl. Cryst.*, **44**, 1272 (2011). DOI: 10.1107/S0021889811038970
- [17] A. Jain, S.P. Ong, G. Hautier, W. Chen, W.D. Richards, S. Dacek, S. Cholia, D. Gunter, D. Skinner, G. Ceder, K.A. Persson. *APL Materials*, **1**, 011002 (2013). DOI: 10.1063/1.4812323
- [18] H.St.C. O'Neill, W.A. Dollase. *Phys. Chem. Minerals*, **20**, 541 (1994). DOI: 10.1007/BF00211850
- [19] S. Sugano, Y. Tanabe. *J. Phys. Soc. Jpn.*, **13**, 880 (1958). DOI: 10.1143/JPSJ.13.880
- [20] R. Famery, F. Queyroux, J.-C. Gilles, P. Herpin. *J. Solid State Chem.*, **30**, 257 (1979). DOI: 10.1016/0022-4596(79)90107-5
- [21] M. Kriens, G. Adiwidjaja, W. Guse, K.H. Klaska, C. Lathé, H. Saalfeld, N.Jb. *Miner. Mh.*, **8**, 344 (1996).
- [22] N.M. Khaidukov, M.N. Brekhovskikh, N.Yu. Kirikova, V.A. Kondratyuk, V.N. Makhov. *Russ. J. Inorg. Chem.*, **67** (4), 547 (2022). DOI: 10.1134/S003602362204009X.

- [23] N.M. Khaidukov, M.N. Brekhovskikh, N.Yu. Kirikova, V.A. Kondratyuk, V.N. Makhov. *J. Lumin.*, **248**, 118942 (2022). DOI: 10.1016/j.jlumin.2022.118942
- [24] R.K. Datta, R. Roy. *J. Am. Ceram. Soc.*, **46**, 388 (1963). DOI: 10.1111/j.1151-2916.1963.tb11757.x
- [25] D.E. McCumber, M.D. Sturge. *J. Appl. Phys.*, **34**, 1682 (1963). DOI: 10.1063/1.1702657
- [26] D.D. Ragan, R. Gustavsen, D. Schiferl. *J. Appl. Phys.*, **72**, 5539 (1992). DOI: 10.1063/1.351951
- [27] J.T. Karpick, B. Di Bartolo. *Nuovo Cimento B*, **7** (1), 62 (1972). DOI: 10.1007/BF02827037
- [28] A.P. Vink, A. Meijerink. *J. Lumin.*, **87–89**, 601 (2000). DOI:10.1016/S0022-2313(99)00308-7
- [29] M. Erdem, G. Ozen, U. Yahsi, B. Di Bartolo, *J. Lumin.* **158**, 464 (2015). DOI: 10.1016/j.jlumin.2014.10.053
- [30] D.L. Wood, G.F. Imbusch, R.M. Macfarlane, P. Kisliuk, D.M. Larkin. *J. Chem. Phys.*, **48**, 5255 (1968). DOI: 10.1063/1.1668202
- [31] G.T. Pott, B.D. McNicol. *J. Solid State Chem.*, **7**, 132 (1973). DOI: 10.1016/0022-4596(73)90145-X
- [32] Y. Tokida, S. Adachi. *J. Appl. Phys.*, **112**, 063522 (2012). DOI: 10.1063/1.4754517
- [33] T. Abritta, N.T. Melamed, J. Maria Neto, F. De Souza Barros. *J. Lumin.*, **18–19**, 179 (1979). DOI: 10.1016/0022-2313(79)90098-X
- [34] R.C. Powell, B. Di Bartolo, B. Birang, C.S. Naiman. In: *Optical Properties of Ions in Crystals*. Ed by H.M. Crosswhite, H.W. Moos (Interscience, New York, 1967), p. 207.

Translated by E.Potapova